Korean J. Chem. Eng., **31**(5), 794-800 (2014)
DOI: 10.1007/s11814-013-0270-x

pISSN: 0256-1115
eISSN: 1975-7220

Study of SO_2 oxidation over V_2O_5/activated carbon catalyst using in situ diffuse reflectance infrared Fourier transformation spectroscopy

Wen Jing*,, Qianqian Guo*,**, Yaqin Hou*, Xiaojin Han*, and Zhanggen Huang*,†**

*State Key Laboratory of Coal Conversion, Institute of Coal Chemistry, Chinese Academy of Sciences, Taiyuan 030001, P. R. China
**University of Chinese Academy of Sciences, Beijing 100049, P. R. China
(*Received 14 October 2013 • accepted 8 December 2013*)

Abstract−The SO_2 oxidation over V_2O_5/AC catalyst was studied using an in situ diffuse reflectance infrared Fourier transformation spectroscopy technique at 120 °C. Results reveal that the surface oxygen groups could neither act as active sites for SO_2 oxidation nor supply the oxygen needed for $V^{V}\leftrightarrow V^{IV}$ redox cycle. The vanadia species and gas phase oxygen are essential for SO_2 oxidation. During SO_2 oxidation over V_2O_5/AC, the surface hydroxyl groups involve in the formation of sulfate species. The role of water vapor in flue gas might be to supplement the hydroxyl groups consumed so that the SO_2 oxidation could continue.

Keywords: V_2O_5/AC, In Situ DRIFTS, SO_2 Oxidation, Oxygen Groups, Water Vapor

INTRODUCTION

Processes for the reduction of SO_2 from stationary sources are among the most investigated in the field of environmental catalysis. Activated carbon/coke (AC) has been recognized as one effective adsorbent and catalyst in adsorptive-catalytic cleaning of stack gases [1-5]. Moreover, modification of AC by metal oxides (V_2O_5, CuO, MnO_x, Fe_2O_3) has been reported to significantly improve its activity toward SO_2 removal [6-11]. Among various types of AC-based catalyst/sorbents, V_2O_5/AC was found to be promising because it shows high SO_2 uptake at stack temperatures (120-200 °C), it is easy to be regenerated under reducing conditions [12,13], the SO_2 removed can be converted into valuable products under mild conditions [12,13], and the SO_2, NO and Hg in flue gas can be removed simultaneously [14,15].

SO_2 removal by V_2O_5/AC consists of a number of steps: adsorption of SO_2 onto the surface, oxidation of SO_2 to SO_3 by O_2 in flue gas over V_2O_5 sites, reaction of SO_3 with H_2O in the flue gas to form H_2SO_4, and storage of H_2SO_4 into the pores of AC. Although much effort has been devoted to elucidating this process [6,16-18], no information is available on the evolution of surface species formed during in situ SO_2 removal. The role of surface oxygen functional groups remains unclear. A detailed investigation of SO_2 oxidation over V_2O_5/AC surface is expected to provide a better understanding of SO_2 removal mechanism.

IR spectroscopy provides information on the nature of bonds formed between adsorbates and the surface of catalyst, which makes it possible to identify and follow the evolution of surface species under different conditions. In situ diffuse reflectance infrared Fourier transform spectroscopy (DRIFTS) is especially useful to explore mechanisms of heterogeneous reactions by providing information on the evolution of surface species. A complete characterization of all reaction products makes it possible for the details of reaction mechanism to be discerned. However, DRIFTS of AC-based catalyst/sorbent has not received much attention due to the difficulty in obtaining IR spectra of these highly opaque samples. Our previous work successfully applied DRIFTS to investigate the mechanism of NO reduction over V_2O_5/AC [19,20], showing the feasibility of DRIFTS to study the interaction between gaseous molecules and AC-based catalyst/sorbent surface.

The overall objective of this work is to study the nature of SO_2 oxidation over V_2O_5/AC surface using in situ DRIFTS to advance the understanding of SO_2 removal. Physical-chemical property is studied to evaluate its influence on SO_2 oxidation. With the information gained, the roles of vanadia species, gas phase oxygen and water vapor are discussed.

EXPERIMENTAL SECTION

1. Catalyst Preparation

An activated carbon (AC) from Xinhua chemical plant was crushed and sieved into 30-60 mesh particles and used as support. The V_2O_5/AC catalyst was prepared by pore volume impregnation of AC using an aqueous solution of ammonium metavanadate (NH_4VO_3) in oxalic acid. After the impregnation, the catalyst was dried at 50 °C for 12 h and then at 110 °C for 5 h, followed by calcination in nitrogen at 500 °C for 8 h. In previous work, there was a general agreement on the convenience of obtaining metal oxides in a high oxidation state to improve its catalytic activity at low temperatures [9,21,22]. Considering that some reduced vanadium species were formed during calcination in presence of carbon [22], the catalyst was preoxidized in a stream of diluted oxygen (3%) at 250 °C for 5 h to obtain more oxidized vanadium species before use. The V_2O_5 loading in catalyst was confirmed to be 1 wt% by ICP. The catalyst is termed as V/AC

†To whom correspondence should be addressed.
E-mail: zghuang@sxicc.ac.cn

for brevity.

2. Desulfurization Measurement

A typical desulfurization measurement was conducted in a fixed-bed quartz reactor (i.d. 22 mm) loaded with 3 g catalyst at 120 °C. Simulated flue gas consisting of 1,500 ppmv SO_2, 4.5% (v/v) O_2, 2.5% (v/v) H_2O and N_2 to balance. H_2O (g) was introduced into the reactor by passing N_2 through a heated gas-wash bottle containing deionized water. The total flue rate was maintained at 400 ml/min yielding GHSV of 4,000 h^{-1}. The concentrations of inlet and outlet SO_2 and O_2 were measured by an on-line flue gas analyzer (KM 9106 Quitox, Kane-May International Limited).

3. Surface Area and Pore Structure Analysis

The textural properties of the samples were measured through nitrogen adsorption at 77 K using ASAP 2020 Micromeritics analyzer. Prior to measurement, the sample was degassed at 150 °C for 10 h. Specific surface area was calculated from the N_2 adsorption isotherms applying Brunauer-Emmett-Teller (BET) equation. The pore size distribution was calculated from desorption branches using BoppJancsoHeinzinger (BJH) method.

4. FTIR Analysis

Fourier transform infrared (FTIR) spectra were recorded on Bruker Tensor 27 FTIR equipped with a high sensitive MCT detector cooled by liquid N_2. The samples were mixed with potassium bromide, ground and palletized. The weight ratio of the sample to potassium bromide was 1 : 300. Sixty-four scans were made and averaged to yield a spectrum with resolution of 4 cm^{-1} over the spectral range 4,000-600 cm^{-1}.

5. In Situ DRIFTS Experiments

In situ DRIFT spectra were recorded on Bruker Tensor 27 FTIR by using an in situ DRIFTS reflection chamber. All experiments were conducted at constant temperature of 120 °C. Mass flow meters and a sample temperature controller were used to control reaction conditions. IR spectra were recorded at a resolution of 8 cm^{-1} for 100 scans. The sample for in situ DRIFTS studies was finely ground and placed into a crucible in the in situ chamber with ZnSe windows. Prior to each experiment, the samples were pretreated at 200 °C in 100 ml/min N_2 for 30 min to blow off water, physisorbed impurities and powder. The chamber was then cooled to 120 °C and kept constant for 5 min. Subsequently, a background spectrum of the sample was recorded. After collecting the background, we conducted the DRIFTS experiments by exposing the pretreated sample to 150 ppmv SO_2 in N_2 or to a mixture of 150 ppmv SO_2, 4.5% (v/v) O_2 with N_2 as carrier to study SO_2 adsorption and oxidation, respectively. In both cases, the flow rate was maintained at 100 ml/min. To avoid influence of water vapor, reactant gases were dried with $CaCl_2$ before being introduced into the chamber. The loss of those species depleted in the surface reactions would show negative bands, whereas those of products positive bands.

To study the effect of water on the oxidation of SO_2, water vapor was added to the reactant feed by passing 50 ml/min N_2 as a carrying gas through an insulated stainless steel bottle filled with distilled water at 45 °C. This feed gas was mixed with the main gas before entering the DRIFTS cell, resulting in a water vapor content of 3% (v/v) with a constant flow rate of 100 ml/min. The DRIFTS experiments were conducted by introducing 3% (v/v) H_2O and 4.5% (v/v) O_2 in N_2 for 10 min before the background spectrum was collected. Then, 150 ppmv SO_2 was introduced in the gas mixture and spectra were recorded at a resolution of 8 cm^{-1} for 100 scans.

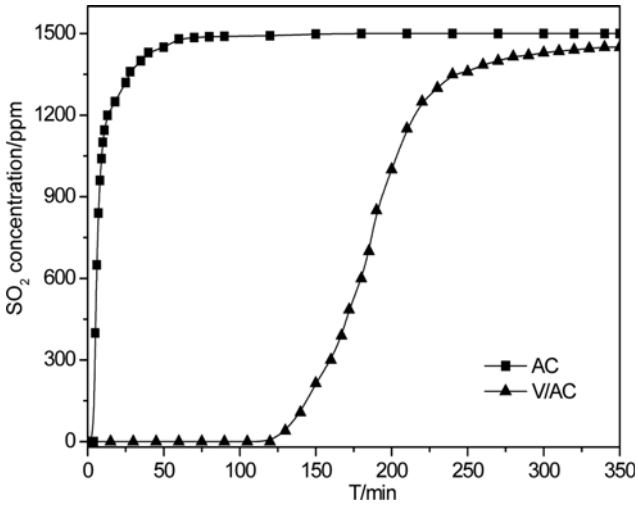

Fig. 1. Breakthrough profiles of SO_2 on AC and V/AC. Reaction conditions: 3 g Cat; 1,500 ppmv SO_2; 4.5% (v/v) O_2; 2.5% (v/v) H_2O; N_2 balance; 4,000 h^{-1}; 120 °C.

RESULTS

1. SO_2 Breakthrough Analysis

Fig. 1 describes the breakthrough characteristics of SO_2 on AC and V/AC. The SO_2 breakthrough on AC occurs instantaneously at the moment SO_2 is introduced, followed by an abrupt increase in the outlet SO_2 concentration up to 1,200 ppm within 5 min. Then, the increase proceeds relatively slowly until outlet concentration of SO_2 reaches inlet value at 60 min, indicating the saturation of AC with SO_2. Compared to that of AC, the breakthrough time of SO_2 on V/AC is observed to increase drastically to 120 min. After the breakthrough point, the outlet SO_2 concentration increases rapidly to a relatively constant value close to inlet concentration. The complete saturation of V/AC with SO_2 is roughly reached until 350 min. The amount of SO_2 adsorbed is quantified by integration of the area below the profile. Results show that AC recorded only 6 mg SO_2/gAC, whereas V/AC showed 102 mg SO_2/gV/AC or 17 times that of AC. The S/V molar ratio of sulfated V/AC is 14.5, indicating that the sulfur-containing species formed mainly exists on AC support. Apparently, the nature of SO_2 interaction with AC surface is significantly changed by the process of loading vanadia species, resulting in drastic enhancement of SO_2 retention.

2. Study of Physical-chemical Property

The SO_2 oxidation over V/AC is expected to be affected by the textural property, the surface chemistry and the vanadia species. The change in physical-chemical property of V/AC relative to that of AC is thus necessary to be studied to evaluate its influence on SO_2 oxidation.

The effect of loading vanadia species on textural property of original AC support is determined by N_2 adsorption-desorption at 77 K, and results are shown in Fig. 2(a). In both cases, the N_2 adsorption isotherms are of type I according to the classification by Brunauer et al. [23], indicative of microporosity. However, the hysteresis loop observed at the relative high pressure suggests the presence of mesopores. It can be appreciated that the adsorption capacity of original

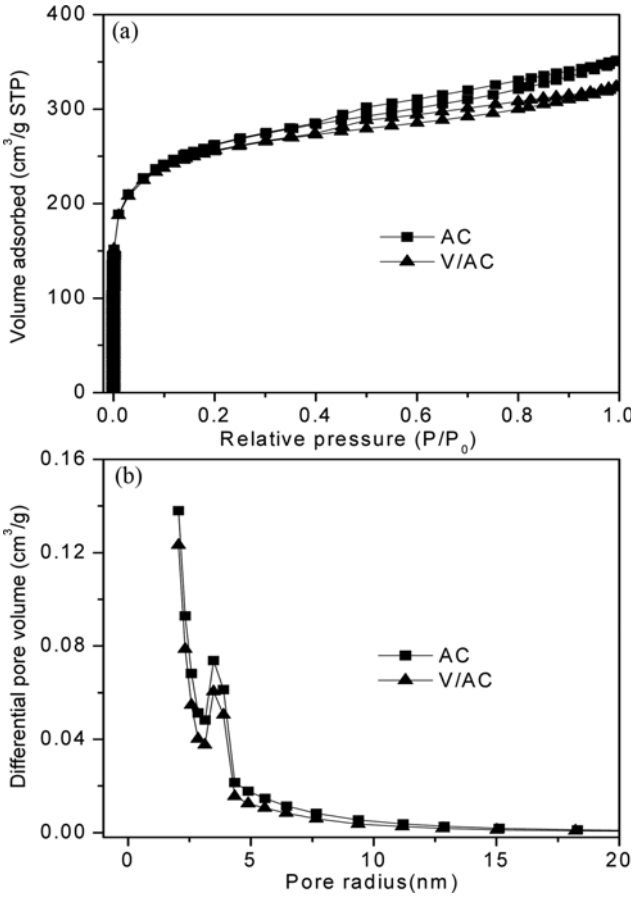

Fig. 2. N_2 adsorption-desorption isotherms (a) and pore size distribution (b) for AC and V/AC.

Table 1. Textural properties of AC and V/AC

Samples	S_{BET} (m^2/g)	V_{total} (cm^3/g)	Average pore width (nm)
AC	910	0.544	2.391
V/AC	884	0.501	2.266

AC support decreases after loading vanadia species due to porous blockage, which is accompanied by a decrease in BET surface area and total pore volume, as shown in Table 1. The effect of loading vanadia species on AC porosity can be clearly appreciated by analyzing pore size distributions. As illustrated in Fig. 2(b), both the micropore (pore radius less than 2 nm) and mesopore (pore radius higher than 2 nm) show slight loss of accessible volume after loading vanadia species, the loss being especially relevant when pores with radius less than 4 nm are considered. The average pore width shows slight decrease after loading vanadia species (Table 1).

A high affinity for SO_2 adsorption on AC is attributed to overlapped absorption potential, which could be weakened with an enlargement of micropore size. Although porous blockage occurs after loading vanadia species, the pore size distribution, especially the micropore size of AC, is not significantly affected. Thus, the change in textural property of AC after loading vanadia species is considered to be insignificant for SO_2 oxidation over V/AC.

To determine the surface chemistry, FTIR spectra of AC and V/AC were collected and shown in Fig. 3. The spectra have similar

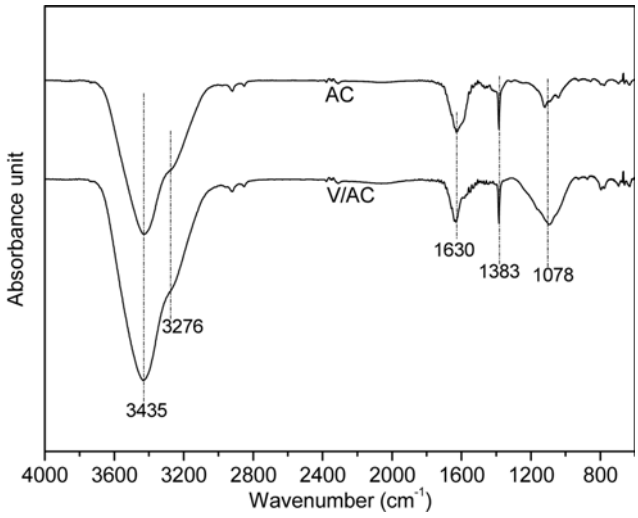

Fig. 3. FTIR spectra of AC and V/AC.

adsorption bands with the difference being in their intensities. The band in the region of 950-1,300 cm^{-1} with feature at 1,078 cm^{-1} is assigned to both C-O stretching and O-H bending modes of alcoholic and carboxylic groups [3,24]. The sharp band at 1,383 cm^{-1} can be ascribed to the -OH bending vibration of phenol [25]. The band at 1,630 cm^{-1} is associated with presence of water adsorbed and/or the highly conjugated C=O groups such as quinones and carbonyl groups near hydroxyl ones [26]. The broad band between 3,000 and 3,650 cm^{-1} with peak at 3,435 cm^{-1} and shoulder at 3,276 cm^{-1} is related to the stretching vibration of hydroxyl, phenolic and carboxylic groups, probably with the participation of water adsorbed on carbon surface [24,27].

Compared with AC, no bands indicating the formation of new types of oxygen functional groups were observed on V/AC. However, the stronger peak intensity of V/AC in comparison with that of AC suggests the bonding of oxygen atom on the AC surface during preoxidation, which enhances the amount of oxygen functional groups existing on AC matrix. All of the oxygen groups determined by FTIR are acidic [28] and have a repulsion effect on the adsorption of acidic gas such as SO_2. Raymundo-Piñero et al. studied SO_2 oxidation over a wide variety of AC and ACF samples with different porosity and surface oxygen content [29], and found that the SO_2 oxidation is inhibited by oxygen complex existing on carbon surface because they block SO_2 access to active sites [29]. Accordingly, although preoxidation in air is favorable to obtain fully oxidized vanadia species, the increase in oxygen content very likely produces negative effect on the SO_2 adsorption and oxidation over V/AC simultaneously.

3. DRIFTS Study on the Nature of SO_2 Interaction with V/AC

3-1. SO_2 Adsorption

The AC and V/AC were exposed to 150 ppmv SO_2 in N_2 to study SO_2 adsorption. The spectra were recorded as a function of time, and are shown in Fig. 4. In both cases, two peaks at 1,345 and 1,373 cm^{-1} that are characteristics of gas phase SO_2 were observed [29]. Within the experimental time of 60 min, no other IR active bands were observed on both AC and V/AC, which implies that there were no other gas products containing sulfur and products in solid phase. When a nitrogen blow-off process was carried out, the two peaks disappeared.

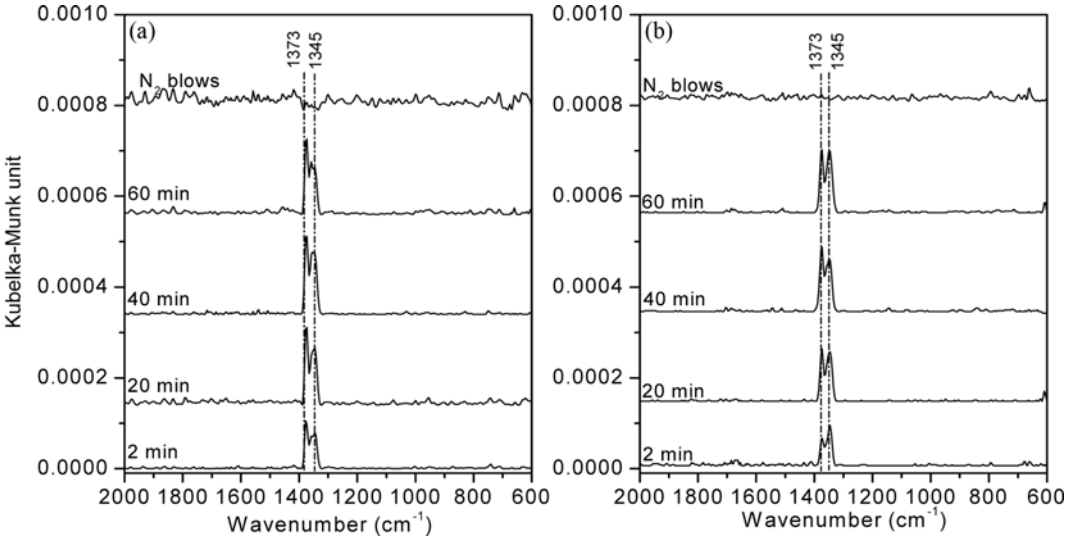

Fig. 4. DRIFTS spectra for AC (a) and V/AC (b) after exposure to 150 ppmv SO_2 in N_2 for 2, 20, 40, 60 min and a subsequent N_2 blow-off process.

It is accepted that the SO_2 oxidation over V_2O_5/AC undergoes a Mars-van Krevelen redox cycle [17,18]. SO_2 was oxidized into SO_3 by vanadium(V) with parallel reduction of vanadium(V) to vanadium(IV). The vanadium(IV) was reoxidized to vanadium(V) by oxygen accompanied with SO_3 leaving vanadium, closing the redox cycle. The absence of detectable peaks assigned to SO_3 or sulfate species indicates that the oxygen needed for the redox cycle over V/AC does not come from the oxygen functional groups on AC surface. Moreover, the oxygen groups could not give its oxygen directly to SO_2 for SO_2 oxidation to take place.

3-2. SO_2 Oxidation

Fig. 5 shows the spectra for AC during exposure to a mixture flow of 150 ppmv SO_2, 4.5% (v/v) O_2 and balanced N_2 at a rate of 100 ml/min. The main features of the spectra are the two peaks at 1,345 and 1,373 cm^{-1} assigned to gas phase SO_2. The SO_3 in gas phase has been reported to have four fundamental vibrations at 532, 652, 1,069 (IR inactive) and 1,390 cm^{-1} [29], which could not be observed until 60 min. This indicates that the oxidation of SO_2 to SO_3 over AC surface occurs to a little extent, although the overlap of intense SO_2 adsorption band might be responsible for no detection of SO_3. This result suggests that surface oxygen groups have little activity transferring gas phase oxygen to SO_2 for its oxidation to SO_3. Additionally, it is observed that some weak bands at 1,560 and 1,650 cm^{-1} became visible, indicating the oxidation of AC surface which results in the formation of carbonyl and hydroxyl groups [24,26].

Fig. 6 shows the in situ DRIFTS spectra during exposure of 150 ppmv SO_2, 4.5% (v/v) O_2 to V/AC. At the beginning of the experiment, the gas phase SO_2 with characteristics at 1,345 and 1,373 cm^{-1} is observed. As the exposure proceeds, the gas phase SO_2 disappears. A broad band in the region 900-1,300 cm^{-1} with features at 978, 1,051, 1,148 and 1,234 cm^{-1} became visible, the peak inten-

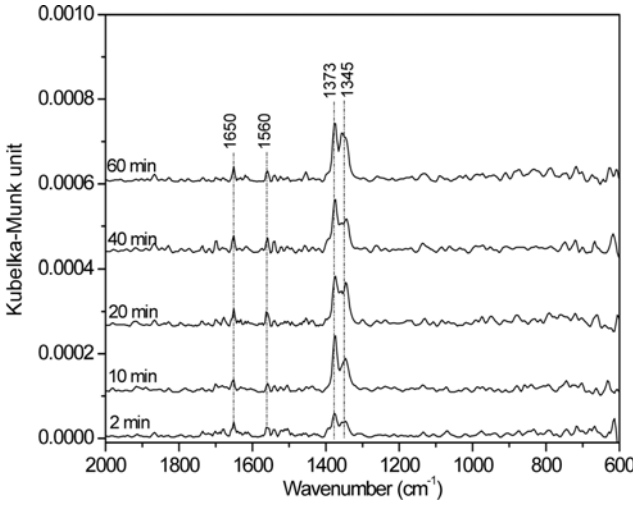

Fig. 5. DRIFTS spectra for AC after exposure to 150 ppmv SO_2 and 4.5% O_2 (v/v) in N_2 for 2, 10, 20, 30, 40 and 60 min.

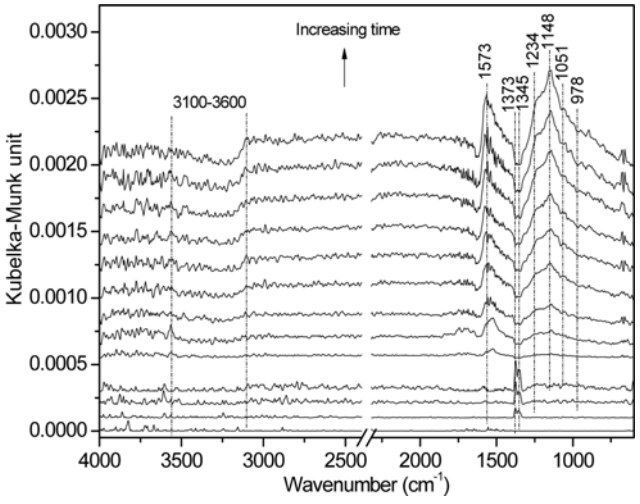

Fig. 6. DRIFTS spectra for V/AC catalyst after exposure to 150 ppmv SO_2 and 4.5% (v/v) O_2 in N_2 for 1, 2, 3, 5, 10, 15, 20, 25, 30, 35, 40, 50 and 60 min.

sity increasing continuously with time. This band is assigned to the stretching motion of adsorbed bisulfate, HSO_4^-, and/or sulfate, SO_4^{2-}, on the surface. As a free anion in solution, sulfate has tetrahedral symmetry and belongs to the point group *Td*. For this symmetry, there are two infrared sulfate vibrations that are accessible to spectroscopic investigation with FTIR technique. They are nondegenerate symmetric stretching ν_1 (980 cm^{-1}, IR inactive) and triply degenerate asymmetric stretching ν_3 bands (1,100 cm^{-1}, IR active). When the sulfate ion is adsorbed on a surface, its symmetry can be lowered into C_{3v} or C_{2v}. As a result, the ν_1 vibration mode becomes IR active, and ν_3 vibration splits into two peaks for C_{3v} and three peaks for C_{2v}. Thus, the broad band in the region 900-1,300 cm^{-1} is a result of ν_1 vibration and ν_3 splitting. This band remains when a blow-off process is carried out, suggesting that the surface-adsorbed species is chemisorbed. Clearly, the gas phase SO_2 transforms into the bound sulfate product which accumulates on the surface of V/AC with time.

Concomitantly with the development of sulfate species, the OH region experiences appearance and progressive increase of a broad negative band from 3,100 to 3,600 cm^{-1}. This band might be attributed to vibrations of surface hydroxyl species, implying that the surface hydroxyl groups very likely involved in the production of HSO_4^{2-} and SO_4^{2-} while they interact with SO_2 in presence of O_2. It is known that there exists a balance between surface hydroxyl groups and water vapor in gas phase. During the desulfurization, the hydroxyl groups consumed could be supplemented by water vapor in flue gas so that the oxidation reaction could continue until carbon support was saturated with sulfate species. This might be the way the water vapor is involved in SO_2 oxidation and sulfuric acid formation, which will be further verified later.

In addition, a band at 1,573 cm^{-1} appears and progressively increases its intensity with the development of sulfates. Previously, the band around 1,580 cm^{-1} was observed by many authors after a surface oxidation of carbon by oxygen, and explained by the stretching vibrations of aromatic C=C which are polarized by the oxygen atoms bound near one of the C atoms [25,30,31]. However, the oxygen oxidation process on activated carbons must be carried out at 300 °C or above to effectively make oxygen to be adsorbed on carbon surface [25,32,33]. The temperature for SO_2 oxidation over V/AC is 120 °C, which is much lower than that required for the formation of adsorbed oxygen atom. Moreover, exposure of V/AC to 4.5% (v/v) O_2 in N_2 only creates some weak bands at 1,560 and 1,630 cm^{-1}, which is similar to that shown in Fig. 5, giving direct indication that the oxidation of carbon surface occurs to a little extent under given conditions. Therefore, adsorbed oxygen atom as a result of carbon surface oxidation resulting in the stretching vibrations of aromatic C=C and the appearance of the band at 1,573 cm^{-1} is very likely unreasonable. A speculation is that the sulfate species formed adsorb on the carbon surface via either one or two of its oxygen atoms, inducing sufficient asymmetry into polyaromatic network to allow IR inactive C=C modes to become active, or increasing the extinction coefficient due to an increase in the dipole moment associated with these ring vibrations. As a result, a band at 1,573 cm^{-1} appears and its intensity increases with the development of sulfate species. This further indicates that the interaction between the sulfate species and V/AC surface is strongly chemisorbed in nature.

3-3. Effect of Water Vapor on SO_2 Oxidation

To further investigate SO_2 oxidation over V/AC under more realistic conditions, the corresponding SO_2+O_2 exposure was conducted in the presence of 3% (v/v) water, as shown in Fig. 7. Moreover, to elucidate the effect of water during SO_2 exposure, IR spectra for V/AC after 60 min of SO_2+O_2 exposure in the absence and presence of water are shown in Fig. 8. We note the difference in intensity of the scale between right and left parts of the graph for the sake of clarity.

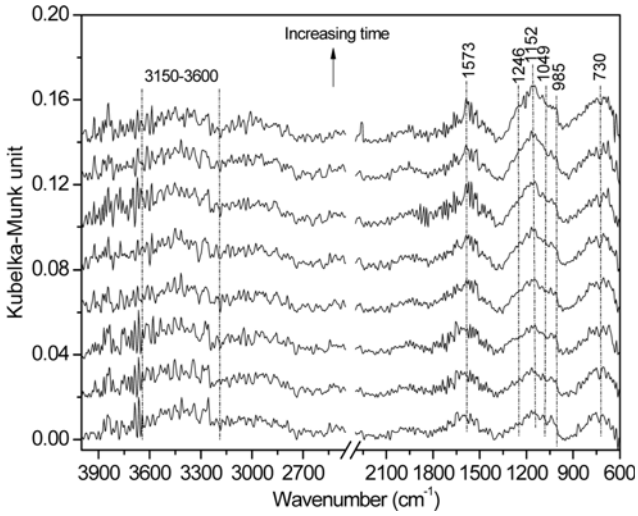

Fig. 7. DRIFTS spectra for V/AC catalyst after exposure to 150 ppmv SO_2, 4.5% (v/v) O_2 and 3% (v/v) H_2O in N_2 for 1, 6, 10, 20, 30, 40, 50 and 60 min.

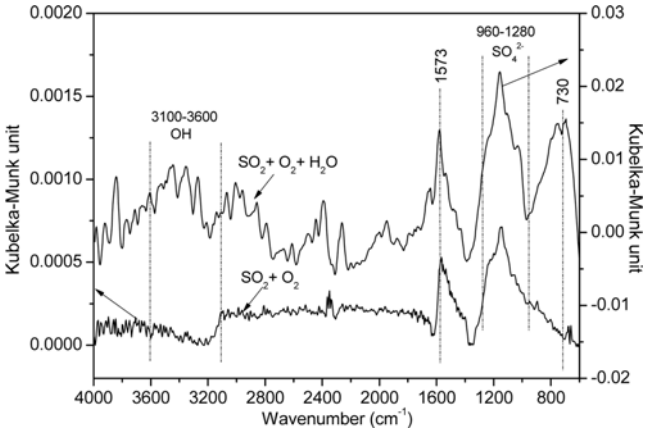

Fig. 8. DRIFTS spectra for V/AC catalyst after exposure to 150 ppmv SO_2 and 4.5% (v/v) O_2 in N_2 in the absence and presence of 3% (v/v) H_2O for 60 min.

As shown in Fig. 7, the addition of water significantly affects SO_2 oxidation. The band in the region 900-1,300 cm^{-1} assigned to sulfate species appears immediately at the moment SO_2 is introduced in the stream. The peak intensity increases with time, the trend being not as apparent as that in absence of water. Comparison of IR spectra in Fig. 8 reveals three obvious differences in the presence of water from that in the absence: (i) the peak intensity of sulfate species in presence of water is 40 times that of in the absence, (ii) the appearance of corresponding positive band in the region 3,100-3,600 cm^{-1}, and (iii) the appearance of new band at 730 cm^{-1}. Difference (i) suggests that water vapor greatly enhances SO_2 oxidation.

Difference (ii) together with the absence of peak at 1,640 cm^{-1} related to O-H-O bending vibration of adsorbed water strongly indicates that the way the water vapor involves in SO_2 oxidation is to form hydroxyl groups which then react with SO_2 to form sulfates, verifying the aforementioned speculation. In the case of difference (iii), however, no S-O vibration in SO_4^{2-} or SO_3^{2-} is expected to give rise to the band at 730 cm^{-1}. The appearance of band at 730 cm^{-1} in presence of water is not fully understood. It may be associated with the complexity of AC surface.

The effect of water on SO_2 oxidation over AC was also performed under the same conditions as that for V/AC. The spectra are rather similar to that for V/AC (not shown for brevity), but the peak intensity is significantly weaker. This indicates that the promotion of water on SO_2 oxidation over AC is independent on the presence of vanadia species. However, the weaker peak intensity reflects the low activity of AC surface for SO_2 oxidation.

DISCUSSION

SO_2 removal on activated carbon/coke (AC) in presence of O_2 and H_2O involves a series of reactions that leads to sulfuric acid as the final product. The rate-determining step in the overall process is oxidation of SO_2 to SO_3. Thus, modification of AC to improve its catalytic activity toward SO_2 oxidation could enhance SO_2 retention. The different behavior of SO_2 over AC and V/AC, as shown in Fig. 5 and 6, clearly shows that the V_2O_5 improves SO_2 oxidation and enhances SO_2 retention, since the change in physical-chemical property during synthesis of catalyst has no positive effect on SO_2 oxidation over AC. The V_2O_5 generally shows catalytic activity at 400 °C or above [34,35], and the low-temperature activity of V_2O_5/AC has been reported to be a result of synergetic role between carbon and vanadia [17]. However, the synergetic role has not been illustrated in detail. In the case of SO_2 oxidation over metal oxide supported vanadia catalysts, SO_2 oxidation activity was found to be apparently related to bridging V-O-M bond (M=metal oxide support) [34,36]. The electronegativity of oxide support cation affects the electron density on bridging V-O-M oxygen: lower cation electronegativity results in higher electron density (more basic V-O-M oxygen) and higher cation electrohegativity results in lower electron density (less basic V-O-M oxygen). A more basic V-O-M bond is considered to be more favorable for SO_2 oxidation. Accordingly, the electronegativity of support greatly affects the nature of vanadia species. Although little information can be available on molecular structure of vanadia species on AC, it is expected that the interaction between carbon, which has low cation electronegativity and acts as an electron donor, and vanadia enhances the electron density of vanadia species, making it more basic and more active towards SO_2 oxidation and leading to V_2O_5/AC catalyst being considerably active toward SO_2 catalytic removal at low temperatures.

Fig. 4(b) and Fig. 6 show that SO_2 oxidation over V_2O_5/AC only takes place in the presence of O_2, suggesting the critical role of O_2. It is accepted that the role of O_2 is to reoxidize V(IV) into V(V) during the redox cycle. However, it is not clear whether adsorption of O_2 on catalyst is an essential step. To clarify this, SO_2 oxidation was performed on V_2O_5/AC preadsorbed with oxygen. No sulfate species could be detected. Thus, the SO_2 oxidation over V_2O_5/AC very likely takes place between adsorbed SO_2 and gas phase O_2, following an Eley-Rideal kinetic model. The SO_2 adsorbed could not be discriminated by DRIFTS due to the very limited SO_2 adsorption and/or that the weak interaction of SO_2 with AC surface makes it difficult to distinguish SO_2 adsorbed from that in gas phase. However, the weakly adsorbed SO_2 on AC and its transformation into SO_3 in presence of O_2 were demonstrated by Raymundo-Piñero et al. using TPD [29]. Similarly, the SO_2 adsorbed was not detected using DRIFTS [29].

Fig. 8 shows that the presence of water vapor significantly enhances SO_2 oxidation over V/AC. It is generally accepted that the role of water vapor is to adsorb on AC and react directly with SO_3 to form H_2SO_4. However, physically adsorbed water was not observed in the presence of water (Fig. 7), indicating the low ability of water to adsorb on AC surface which is hydrophobic in nature at the reaction temperature of 120 °C. Thus, water vapor involving in SO_2 oxidation likely contains a first step where it chemically adsorbs on AC via forming hydroxyl groups, which are more thermally stable and react with SO_2 to form sulfates, as demonstrated in Fig. 6. However, the nature of the hydroxyl group involved in SO_2 oxidation and its interaction with SO_2 to form sulfates could not be exactly determined on the basis of data in present paper. More specific studies will be carried out in forthcoming research.

CONCLUSIONS

The nature of SO_2 oxidation over V_2O_5/AC catalyst was investigated using in situ DRIFTS method. Results show that the vanadia species, rather than the certain change in physical-chemical property of AC, significantly improves SO_2 oxidation and retention. The surface oxygen groups could neither act as active sites for SO_2 oxidation nor supply the oxygen needed for $V^{V} \leftrightarrow V^{IV}$ redox cycle. Gas phase oxygen and vanadia species are essential for SO_2 oxidation. The SO_2 oxidation over V_2O_5/AC follows an Eley-Rideal kinetic model involving adsorbed SO_2 and gas phase oxygen and leads to formation of sulfate as final product. The surface hydroxyl groups play an important role in the formation of sulfate species. During desulfurization, the water vapor in flue gas could supplement the hydroxyl groups consumed so that the SO_2 oxidation could continue until AC support becomes saturated. In this way, the water vapor greatly enhances SO_2 removal.

ACKNOWLEDGEMENTS

The National Natural Science Foundation of China (21106174, 21103218, 21177136), International Cooperation of Shanxi Province (2012081019) and Strategic Priority Research Program of the Chinise Academy of Sciences (XDA07030300) are acknowledged.

REFERENCES

1. Y. Guo, Y. Li, T. Zhu and M. Ye, *Energy Fuels*, **27**, 360 (2013).
2. J. M. Rosas, R. Ruiz-Rosas, J. Rodríguez-Mirasol and T. Cordero, *Carbon*, **50**, 1523 (2012).
3. Y. Zhu, J. Gao, Y. Li, F. Sun, J. Gao, S. Wu and Y. Qin, *J. Taiwan Inst. Chem. Eng.*, **43**, 112 (2012).
4. Y. Zhu, J. Gao, Y. Li, F. Sun and Y. Qin, *Korean J. Chem. Eng.*, **28**, 2344 (2011).

5. F. Sun, J. Gao, Y. Zhu and Y. Qin, *Korean J. Chem. Eng.*, **28**, 2218 (2011).
6. Y. Xiao, Q. Liu, Z. Liu, Z. Huang, Y. Guo and J. Yang, *Appl. Catal. B: Environ.*, **82**, 114 (2008).
7. H.-H. Tseng and M.-Y. Wey, *Carbon*, **42**, 2269 (2004).
8. J. Ma, Z. Liu, S. Liu and Z. Zhu, *Appl. Catal. B: Environ.*, **45**, 301 (2003).
9. G. Marbán and A. B. Fuertes, *Appl. Catal. B: Environ.*, **34**, 55 (2001).
10. D. Loìpez, R. Buitrago, A. Sepuìlveda-Escribano, F. Rodriìguez-Reinoso and F. Mondragoìn, *J. Phys. Chem. C*, **112**, 15335 (2008).
11. Y.-F. Qu, J.-X. Guo, Y.-H. Chu, M.-C. Sun and H.-Q. Yin, *Appl. Surf. Sci.*, **282**, 425 (2013).
12. X. Xing, Z. Liu and J. Yang, *Fuel*, **87**, 1705 (2008).
13. Y. Guo, Z. Liu, Q. Liu and Z. Huang, *Catal. Today*, **131**, 322 (2008).
14. J. Wang, J. Yang and Z. Liu, *Fuel Process. Technol.*, **91**, 676 (2010).
15. Y. Wang, Z. Liu, L. Zhan, Z. Huang, Q. Liu and J. Ma, *Chem. Eng. Sci.*, **59**, 5283 (2004).
16. J. Ma, Z. Liu, Q. Liu, S. Guo, Z. Huang and Y. Xiao, *Fuel Process. Technol.*, **89**, 242 (2008).
17. Z. Zhu, Z. Liu, H. Niu, S. Liu, T. Hu, T. Liu and Y. Xie, *J. Catal.*, **197**, 6 (2001).
18. E. García-Bordejé, J. L. Pinilla, M. J. Lázaro and R. Moliner, *Appl. Catal. B: Environ.*, **66**, 281 (2006).
19. D. Sun, Q. Liu, Z. Liu, G. Gui and Z. Huang, *Appl. Catal. B: Environ.*, **92**, 462 (2009).
20. D. Sun, Q. Liu, Z. Liu, G. Gui and Z. Huang, *Catal. Lett.*, **132**, 122 (2009).
21. Y. Wang, Z. Huang, Z. Liu and Q. Liu, *Carbon*, **42**, 445 (2004).
22. Z. Zhu, Z. Liu, S. Liu and H. Niu, *Appl. Catal. B: Environ.*, **23**, L229 (1999).
23. S. Brunauer, L. S. Deming, W. E. Deming and E. Teller, *J. Amer. Chem. Soc.*, **62**, 1723 (1940).
24. A. Zhou, X. Ma and C. Song, *Appl. Catal. B: Environ.*, **87**, 190 (2009).
25. E. García-Bordejé, M. J. Lázaro, R. Moliner, P. M. Álvarez, V. Gómez-Serrano and J. L. G. Fierro, *Carbon*, **44**, 407 (2006).
26. A. Pigamo, M. Besson, B. Blanc, P. Gallezot, A. Blackburn, O. Kozynchenko, S. Tennison, E. Crezee and F. Kapteijn, *Carbon*, **40**, 1267 (2002).
27. M.-X. Wang, Z.-H. Huang, K. Shen, F. Kang and K. Liang, *Catal. Today*, **201**, 109 (2013).
28. H. P. Boehm, *Carbon*, **32**, 759 (1994).
29. E. Raymundo-Piñero, D. Cazorla-Amorós and A. Linares-Solano, *Carbon*, **39**, 231 (2001).
30. H. P. Boehm, *Carbon*, **40**, 145 (2002).
31. C. Moreno-Castilla, M. V. López-Ramón and F. Carrasco-Marín, *Carbon*, **38**, 1995 (2000).
32. J. Jaramillo, P. M. Álvarez and V. Gómez-Serrano, *Fuel Process. Technol.*, **91**, 1768 (2010).
33. J.-H. Zhou, Z.-J. Sui, J. Zhu, P. Li, D. Chen, Y.-C. Dai and W.-K. Yuan, *Carbon*, **45**, 785 (2007).
34. J. P. Dunn, P. R. Koppula, H. G. Stenger and I. E. Wachs, *Appl. Catal. B: Environ.*, **19**, 103 (1998).
35. A. Christodoulakis and S. Boghosian, *J. Catal.*, **215**, 139 (2003).
36. J. P. Dunn, H. G. Stenger Jr. and I. E. Wachs, *Catal. Today*, **51**, 301 (1999).